

Walnut Creek HEC-6 Modeling - Sediment Data Analysis and Suggested Sediment Model Parameters

by Allen Teeter, CHT;

15 August 2010

Project Setting

The Walnut Creek basin drains an area of 146 square miles in California and empties into Suisun Bay. The flood control project at the downstream end of the Walnut Creek was constructed in 1965. By 1970, the downstream 3.5 miles had filled in with approximately 1,060,000 yd³ of fine-grained sediment. Although the operation and maintenance manual required the project sponsor, CCCFC&WCD, to remove excess sediments from this reach of the channel, the Corps conducted a one-time dredge of the lower 2.7 miles of the newly constructed channel in 1973. Since the 1973 dredging, the local sponsor has not been able to secure the necessary environmental approvals to conduct additional dredging operations to maintain the advertised capacity of the channel.

As part of general re-design of the project, thirty sediment cores were collected in October 2009 and analyzed to characterize the sediment material which has deposited in the project and to provide information for a model study. The data developed from those sediment cores are summarized here, analyzed, and sediment model parameters suggested.

Walnut Creek empties into Suisun Bay which causes the lower reach to be a sub-estuary of the San Francisco Bay system. Water samples from Sept and Oct 2007 confirmed elevated salinity (specific conductance) values at some downstream locations. Appreciable estuarine sedimentation can occur as the result of sediment transport from seaward, gravitational circulation, and asymmetric tidal transport. Estuarine areas are also generally efficient traps for fine sediments entering from upland.

The magnitude of the suspended load of Walnut Creek is large and may account for the bulk of the shoaling in the project. However, even without a riverine sediment source, appreciable shoaling would occur in the lower reach of this project setting as the result of estuarine sedimentation. Therefore, some background on local estuarine sedimentation is provided below.

Estuarine Aspects of the System

The following paragraphs describe local estuarine and sedimentation conditions. ¹Suisun Bay is located in northern San Francisco Bay, where freshwater from the Sacramento - San Joaquin Delta meets saline water from the Pacific Ocean. Suisun Bay is the furthest landward sub-embayment of San Francisco Bay, and is therefore most responsive to freshwater flow. Most probably, recent water withdrawals from the Delta have caused salinities to increase. Channels in Suisun Bay are about 9-11 m deep. Carquinez Strait is a narrow channel about 18 m deep that connects Suisun Bay to San Pablo Bay, to the rest of San Francisco Bay, and to the Pacific

¹ Ganju, N.K., Schoellhamer, D.H., and Younis, B.A. (2006). "Development of a decadal-scale estuarine geomorphic model for Suisun Bay, California: calibration, validation, and idealized time-stepping," Univ. of Cal. Water Resources Center, Techn. Completion Report, Univ. of California.

Ocean. Tides are mixed diurnal and semidiurnal and the tidal range varies from about 0.6 m during the weakest neap tides to 1.8 m during the strongest spring tides. Freshwater inflow typically first encounters saltwater in the lower rivers, Suisun Bay, and Carquinez Strait. The salinity range in this area is about 0-25 ppt and depends on freshwater inflow. Suisun Bay consists of two smaller sub-embayments, Grizzly and Honker Bays. See Figure 1.

Suspended and bed sediment in Suisun Bay is predominately fine and cohesive, except for sandy bed sediment in some of the deeper channels. The typical suspended-sediment concentration (SSC) range in northern San Francisco Bay is about 10-300 mg/L and sometimes up to about 1,000 mg/L in an estuarine turbidity maximum (ETM). In Suisun Bay, ETMs are located near sills and sometimes near a salinity of 2 ppt, depending on tidal phase and the spring/neap tidal cycle.

An annual cycle of sediment delivery and redistribution begins with large influx of sediment during winter (delivery), primarily from the Central Valley. Much of this new sediment deposits in San Pablo and Suisun Bays. Stronger westerly winds during spring and summer cause wind-wave resuspension of bottom sediment in these shallow waters and increase SSC. The ability of wind to increase SSC is greatest early in the spring, when unconsolidated fine sediments can easily be resuspended. As the fine sediments are winnowed from the bed, however, the remaining sediments become progressively coarser and less erodible. Thus, tides and wind redistribute the annual pulse of new sediment throughout the Bay. Since 1850, alterations in the watershed and estuary have changed the bathymetry of Suisun Bay (see Figure 2).

Recently-deposited sediment beds have been described for Suisun Bay.² Gravity cores obtained in 1990-1991 and 1999 were analyzed to delineate depositional environments and sedimentation patterns in Suisun Bay. Major depositional environments include: tidal channel (sub-tidal), tidal channel banks (sub-tidal), tidal flat (intertidal to sub-tidal), and bay mouth (sub-tidal). The tidal channel environment includes both large and small channels in Suisun Bay as well as the tidal sloughs Suisun and Montezuma Sloughs. The coarsest sediment, usually sand or muddy sand, characterize this environment and water depths range from 2 to 11 m.

Thin (1-2 mm) and discontinuous silt and clay laminae are common. Suisun and Montezuma Sloughs are the exception to this pattern in that they consist of massive, intensely bioturbated muds. Tidal channel banks (both "cut" and "accretionary" channel margins), particularly accretionary banks, are characterized by low-to-moderate bioturbation and sandy mud to muddy sand lithology. Typically alternating sand and mud beds (1-6 cm thick) are present; both types of beds consist of 1 mm to 1 cm thick sub-horizontal to inclined laminae. Laminae composed of organic detritus are also present. Where this environment is transitional with the tidal flat environment water depths range from 2-8 m. Tidal flat environments include the "sand" shoals present on bathymetry charts, and are typically a bioturbated muddy sand to sandy mud. Sand and mud beds, 1-3 cm thick, are often characterized by very fine 1-2 mm thick silt and mud laminae. Water depths range from 2 to 4.5 m where these laminated tidal flat sediments occur.

² Chin, J.L., Orzech, K., Anima, R., and Jaffe, B. (2002). "Modern Estuarine Sedimentation in Suisun Bay, California", American Geophysical Union, Fall Meeting 2002, abstract.

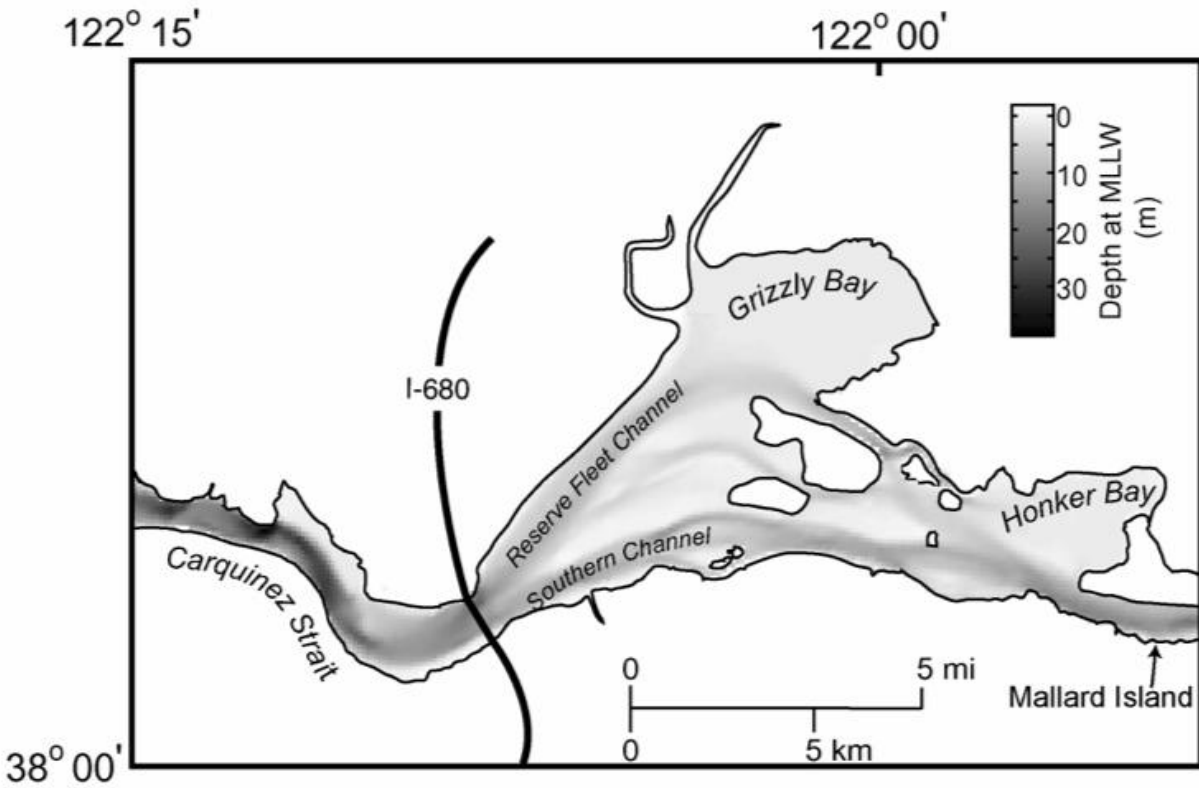


Figure 1. Bathymetry of Suisun Bay (Walnut Creek enters near the “Southern Channel” label).

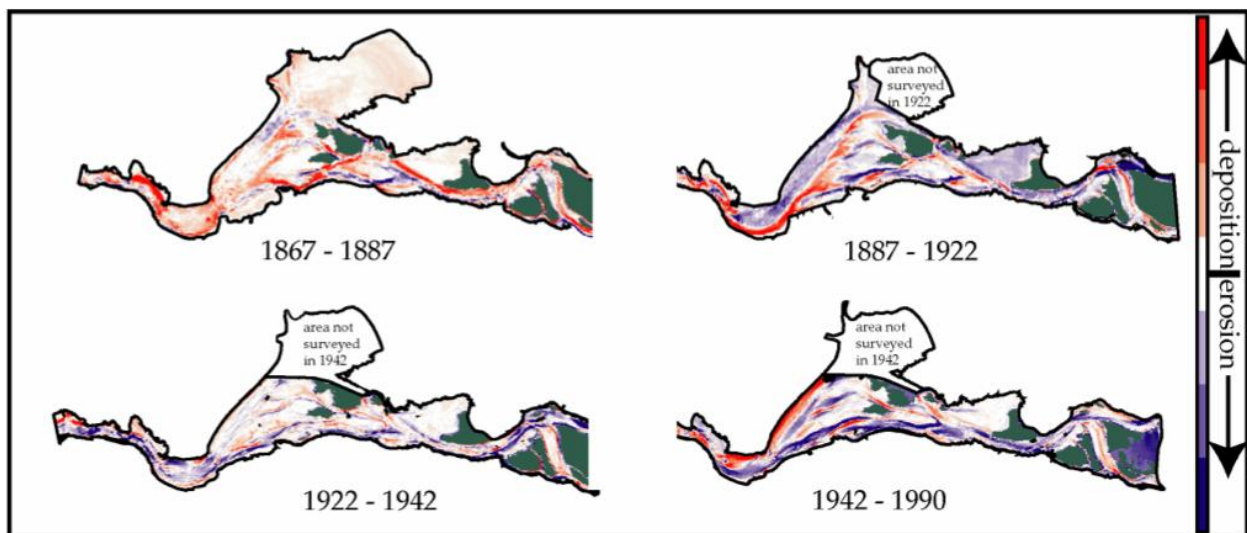


Figure 2. Historical sedimentation patterns in Suisun Bay.

Bay mouth environments occur only in the distal portions of Grizzly and Honker Bays, sub-embayments of Suisun Bay proper. This environment is transitional with both tidal channel bank and tidal flat environments and shares characteristics with each. Massive to interbedded mud is the most common lithology, although sandy mud to muddy sand also occurs. Centimeters thick sand and mud beds typically alternate vertically. Bioturbation is low to moderate. Water depths over this environment range from 2 to 3 m.

Depositional environments present in Suisun Bay are the result of a full range of tidal and fluvial processes as shown by the lithologies and alternating sediment stratigraphic patterns observed in cores. Very thin beds and intense bioturbation evidence intervals of very slow to negligible sedimentation. Rapid deposition and/or resuspension are evidenced by thick sediment intervals and by laminae that are continuous and apparently unbioturbated.

USGS researchers summarized Suisun Bay historical sedimentation patterns as follows³:

- Between 1867 and 1887, approximately 115 million cubic meters of sediment was deposited in the Suisun Bay area. This is equivalent to about 2.5 cm/yr accumulation over all of Suisun Bay. Almost two-thirds of Suisun Bay was depositional during this period. Most of this is debris from hydraulic gold mining in the Sierra Nevada, and is likely contaminated with mercury which was used to extract gold from tailings.
- Hydraulic mining ceased in 1884, while water distribution and flood control projects increased during the 20th century. These factors decreased the input of sediment to the Bay, and from 1887 to 1990 Suisun Bay was erosional.
- On average, Suisun Bay deepened during the study period. From 1867 to 1990, Suisun Bay lost more than 100 million cubic meters of sediment. This is equivalent to a loss of 74 cm over the entire Suisun Bay area.
- Changes in sedimentation in Suisun Bay affected its ecosystem in many ways. For example, the area of tidal flat, rich habitat, and sources of sediment to the wetlands increased by approximately 10 square km from 1867 to 1887 due to the input of hydraulic mining debris. From 1887 to 1990, however, tidal flat area decreased from 52 square km to 12 square km.

There are numerous tidal creeks near the local project area in Suisun Bay which drain tidal marshes. These tidal creeks are expected to be stable with inlet areas balanced by tidal prisms. If this local relationship were known it might be used to make some simple estimates of estuarine shoaling in systems where the inlet is initially larger than the stable size.

There are constructed canals on the south side of Suisun Bay at Port Chicago (or Bay Point?) east of the arsenal. These might provide case studies of the extent of estuarine shoaling. CCCFC&WMD conducted surveys in Lower Walnut Creek but only typical sections were plotted in COE drawing DE-4-137. Water years 1966 and 1968 were low-flow and very low

³ Cappiella, K., Malzone, C., Smith, R.E., and Jaffe, B.E. (1999.) "Historical bathymetric change in Suisun Bay 1867 - 1990," USGS Open-file Report 99-563.

sediment yield years on Walnut Creek. If more detailed survey information were available, an estimate of estuarine shoaling might be made using volume differences between 1967 and 1968 or 1965 and 1966 surveys.

Selenium is a waste product from numerous refineries along Suisun Bay and Carquinez Strait. Most Se attaches to fine sediment particles and to their organic coatings. About 90 percent of selenium directly input to a constructed wetland was trapped.⁴ Subsequently, about 10 to 30 percent was found to be volatilized by wetland plants. The vertical distributions of elevated Se in wetland sediments at Martinez Regional and Benicia State Parks were determined to be fairly uniform by Zawislanski et al.⁵ It might be possible to use Se as a tracer to determine the extent of estuarine shoaling in Lower Walnut Creek if no refinery effluent was input there at least since 1965, and if the magnitude of dissolved Se flux to sediments could be determined.

Some Field Observations

Allen Teeter accompanied the field crew on 20 and 21 October 2009 as they collected most of the recent core samples. Both Kinnetic Laboratory and Hultgren-Tillis Engineers personnel were well experienced and efficient at this work. Few if any fine laminae were observed in the cores at the sampling sites. Some relatively fine inter-bedding was observed near the bottoms of cores VC14 and VC15 that resembled bottom sets. These cores had beds as thin as about 0.1 ft.

Active wetland sedimentation was observed on marsh surface in the lower reach. On the west side of the Lower Walnut Creek reach from Suisun Bay to Waterfront Road (lower-Lower Walnut Creek) fringing marsh about 1000 ft wide is present. This marsh appears to tidally flood and ebb through lower-Lower Walnut Creek. Perhaps this is responsible for the higher deposition along the fringing marsh as compared to the east side of the channel. Riverine-looking channel bars were observed in the middle reach between Waterfront Road and the A. T. & S. F. Railroad bridge.

Hydrocarbon smells and color were evident in some lower-reach cores. Jerrold Hanson indicated that some large spills had occurred in the past and had been used to mark and date core layers in some cases.

It appeared that the recently excavated area in the upper reach (near VC20) had been overlain with 0.25 to 0.75 ft of fine-grained deposits. Some gravel-sized material was observed in this area which was very angular and appeared un-weathered. It was suggested that a local aggregate plant might be the source of this material.

Summary of Core Sediment Data

⁴ Hansen, D., Duda, P.J., Zayed, A., and Terry, N. (1998.) "Selenium removal by constructed wetlands: role of biological volatilization," *Environ. Sci. Technol.*, 32, pp. 591-597

⁵ Zawislanski, P.T., Mountford, H.S., Gabet, E.J., McGrath, A.E., and Wong, H.C. (2001.) "Selenium distribution and fluxes in intertidal wetlands, San Francisco Bay, California," *J. of Environ. Qual.*, 30, pp. 1080-1091.

Kinnetic Laboratories collected 30 cores along Lower Walnut Creek, Hultgren-Tillis Engineers (HTE) logged and sub-sampled the cores⁶ and sent selected samples to Soil Control Lab for analyses. Eighty sub-samples were collected in the field and forty samples were analyzed. Results are summarized in Table 2.

Sediment Size Classifications

A combination of sieve and hydrometer was used to determine the complete grain size distributions of the samples. A triangular graph of the sand, silt, and clay fractions of samples is presented in Figure 3. Color-coded points represent lower, middle and upper Lower Walnut Creek reaches as defined on the figure title. As can be seen, all three reaches are represented across the dimensions of the figure. Only sand was well sorted and clay and silt occurred in roughly equivalent proportions. When plotted as individual distributions, as in Figure 4, silt and clay contents are normally distributed while sand content is log-normally distributed. (This might suggest that silt and clay occur randomly together and sand occurs as the result of hydrodynamic processes or other processes that result in log-normal distributions.)

Twenty percent of the samples analyzed had sand content greater than 50 percent. However, these were not truly random samples as some were selected as representative of certain observed bed classifications. Peats were not selected for analysis because of the difficulties they bring to analyses. The lower reach was sampled much more than the others. Statistics on core sample sand content by project reach is included in Table 5.

A description of the size distribution statistics is presented later.

Sand and Peat Extent in Core Logs

Some 179.4 ft of length in 30 cores were visually classified in the field. Those classified as sand or peat beds are summarized in Table 1 by length in the core logs. Statistical distributions (all log-normal) of all, sand and peat beds are presented in Figure 5. The trend is that sand content increases from downstream to upstream - as supported by the sample data.

Atterberg Limits

Results of these twenty four analyses covered the same range as recorded in the visual classifications: lean to fat clays. Most samples were lean clays with liquid limits below 50 percent. Scatter plots of Atterberg limits and clay content are presented in Figure 6. As can be seen, clay content correlates well with these parameters. Plasticity index and liquid limit are also plotted in Figure 7 in the geotechnical manner suggested by Casagrande and others. These data indicate a comparatively high resistance to erosion (medium to high plasticity). Liquid limit and plasticity index correlate well to clay content (Figure 6) but no spatial difference suggesting a difference in clay type could be detected in the data.

⁶ Hultgren-Tillis Engineers. (Nov 2009.) "Sediment core sampling Lower Walnut Creek Channel Contra Costa County, California," Letter Report to CCCPWFC&WCD, Martinez, California.

Derived Sediment Concentration Parameters

Various sediment parameters were measured on forty core sub-samples. These data were used to derive other parameters as described in this section.

The sample bulk wet density $BWD(w/v) = C_v p_s + (1 - C_v) p_l$ where p_l is the liquid density (w/v), C_v is volume concentration (v/v), and p_s is the particle density (w/v). Other concentration measures are concentration by weight C_w and unit dry weight (or dry density or dry solids content) C_s . Conversions between parameters include the following:
 $C_v = C_s / p_s$ and $C_w = p_s C_v / BWD$.

The average particle density was estimated for a mixture of organic and mineral grains as

$$\frac{1}{\rho_s} = \frac{O_f}{1050} + \frac{(1 - O_f)}{2650}$$

where O_f is the organic fraction and 1050 and 2650 kg/cu m are the assumed organic and particle densities, respectively. Sample organic fraction varied between 0.6 and 4.1 percent (median of 3.05 percent). Average particle densities varied accordingly between 2494 and 2626 kg/cu m (median 2532 kg/cu m).

Pore fluid densities were estimated using the method of Knudsen (1901) assuming that the determinations of pore fluid total dissolved solids (w/v) were equivalent to salinity (w/w). This assumption and since carbonate, bromine and iodine were not separately determined, introduced a small error on the order of 0.1 ppt. Knudsen's method assumes that the salinity-to-chlorinity ratio is 1.80655 and the method is third order in chlorinity and temperature. A temperature of 22 degrees was assumed. Pore fluid total dissolved solids TDS varied between 4.4 and 19.0 g/l (median of 12.0 g/l) and estimated pore fluid density ranged from 1001.2 to 1012.2 kg/cu m (median of 1006.9 kg/cu m).

Sample C_w was estimated by Soil Control Lab from moisture content w determinations. Since $w = (W_{sat} - W_s) / W_s$ (where W_{sat} is the saturated weight and W_s is solids weight in the sample), $C_w = 1 / (w+1)$. The $BWD = p_s p_l / (p_s - C_w (p_s - p_l))$ using the parameters calculated earlier. Then $C_s = C_w BWD$.

Core data was used to estimate representative values of unit dry weights for sand S_a , silt S_l , and clay C_a such that $1 / C_s(total) = C_a(w/w) / C_s(ca) + S_l(w/w) / C_s(sl) + S_a(w/w) / C_s(sa)$ where w/w is the weight fraction and $C_s(ca, sl, sa)$ are the components of total unit dry weight $C_s(total)$. General linear model and least squares fits were attempted but finally an end-member/trial and error method was used to fit the data. (Problems arose apparently because clay and silt unit weights were inversely related to their percentage values while sand was directly related to it.) The result is presented in Figure 8 suggesting representative dry unit weights for clay $C_a = 484$, silt $S_l = 1314$, and sand $S_a = 1811$ kg/cu m. A Pearson's correlation coefficient between total unit dry weights and an estimates of total unit dry weight based on the combination of clay, silt,

and sand unit dry weights was 0.90. The regression forced through 0.0-0.0 yielded an $R^2 = 0.98$ and a standard error of estimate of about 2.2 percent.

Table 2 presents a summary of measured and derived parameters. Scatter plots of concentration parameters and clay, silt, and sand contents are presented in Figures 9 and 10.

Sediment Size Distributions

Cumulative grain size distributions on 40 samples were determined by Soil Control Lab, as previously described, and presented in graphical form. Those plots were digitized at the 16, 31, 50, 69, and 84 percentiles less-than as phi values ($-\log_2(\text{diameter, mm})$). Then statistical methods similar to those of Folk (but generalized to include five points instead of three) were used to estimate mean, sorting (standard deviation), and skewness of distributions. Basing statistics on phi values makes these statistics similar to geometric statistics of mean, etc. On many digitized curves, the 16th percentile lay below the measured points. In most cases the necessary extrapolation was a relatively short interval and was facilitated by the last three measured values. In a couple of cases, extrapolation was more appreciable, almost to the end of the plotted size range.

Size distribution statistics are presented in Figure 11 plotted against channels station. Mean sizes there were converted from phi units back to millimeters. Positive skewness is toward the fine end of the distribution. Over Lower Walnut Creek, sediments in the reach between the mouth (channel station 0+00 or 0.0 in the plot) and 100 (100+00 ft or ft/100) were finer than the remainder of the samples (95% confidence level, p-value = 0.026, and means of 7.5 and 22.6 μm , respectively). Differences in sorting and skewness were small and not significant.

Within the sediment cores, size distribution means (mm) decreased with depth into the sediment (p-value = 0.119), more significantly decreased with water depth at the sampling site (p-value = 0.025) and most significantly with depth in sediment plus water depth (p-value = 0.007). This could indicate that sediments are upward coarsening with respect to the sediment column and the constructed project base (since cores were designed to cover the sediment thickness to the constructed base). This could also reflect that the (coarser) sediments sampled upstream are at a higher elevation (often water depth = 0.0 ft) than the downstream sediments. Scatter plots are presented in Figure 12.

Though there is a clear upstream coarsening, there is also considerable variability in the grain size statistics among the three reaches bounded by Waterfront Road and the A.T. & S. F. Railroad bridge. All three reaches contain some coarse, well sorted, positively skewed samples. See Figure 13. Likewise they also contain fine, poorly-sorted, and more negatively skewed sediments. The former are lag deposits and at channel station 0+00 likely originated from wind-wave transport along the Suisun Bay shoreline.

There are eight combinations of mean, sorting, and skewness when each is considered to either increase or decrease ($2*2*2$). Of these eight, two combinations have been used to infer transport paths in directions of deposition and erosion. To apply this method, many surficial bed samples are usually collected along lines from material that is or recently has been in transport at the

sediment surface. In the case of the Lower Walnut Creek samples, trend in statistics were examined along channel stations. Sediments in the lower reach appear to fine in the upstream direction although the trend is weak (p-value = 0.29). If the three coarsest (and well-sorted and positively skewed) samples are omitted from the analysis, the upstream fining trend improves (p-value = 0.18) and upstream sorting improves (decreases) (p-value = 0.32) and upstream skewness is more negative (p-value = 0.09).

Upstream estuarine transport might be indicated for the lower-Lower Walnut Creek but, as indicated, the trends in sediment statistics are somewhat weak (about 80% confidence level). Statistics and trends are plotted in Figure 14 and an example hypothetical series of differential grain size distributions with the same trend is presented in Figure 15.

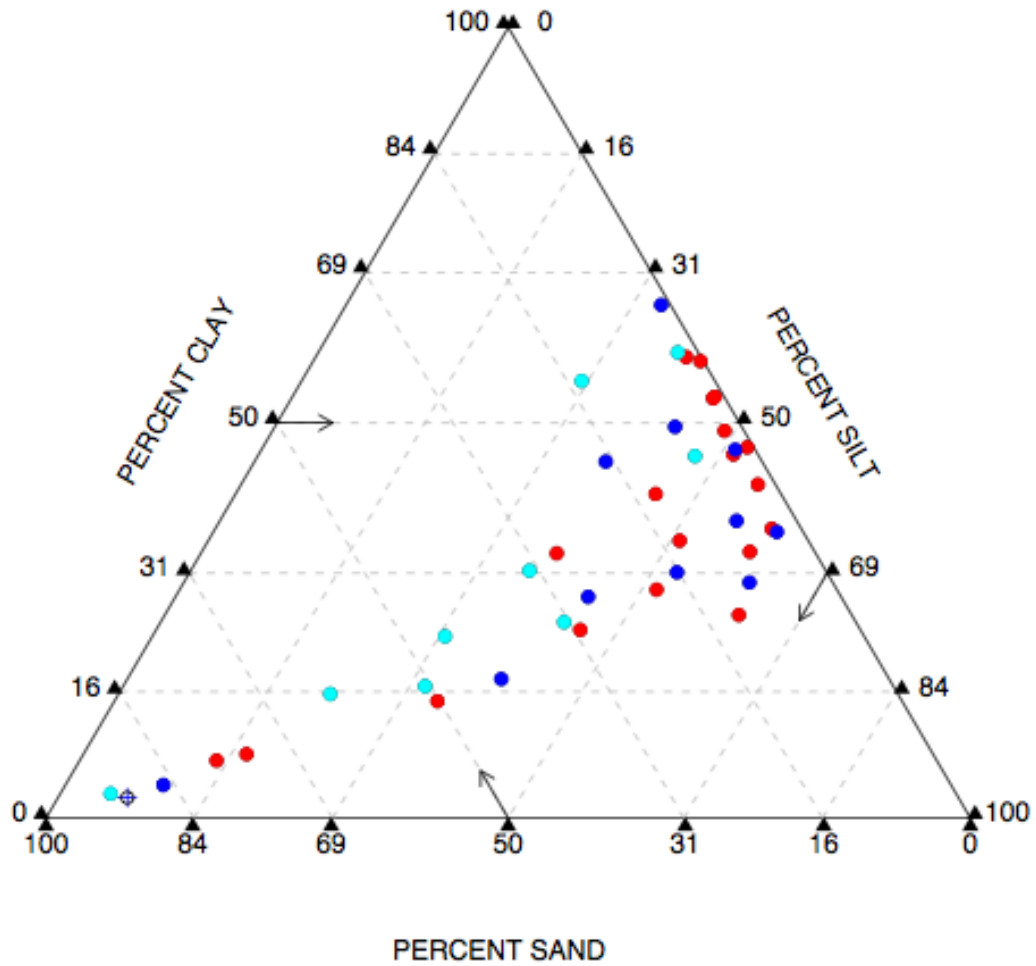


Figure 3. Triangular graph of sand, silt and clay content of Walnut Creek core sub-samples. Read percentages 30 degrees to left of normals to axes as indicated by arrows. Red dots are from below Waterfront Road (HTE, Plate 1), blue dots are between Waterfront Road and A.T. & S. F. Railroad Bridge, and light blue dots are from above the bridge (blue circle with cross in the bottom left corner had gravel content added to sand content).

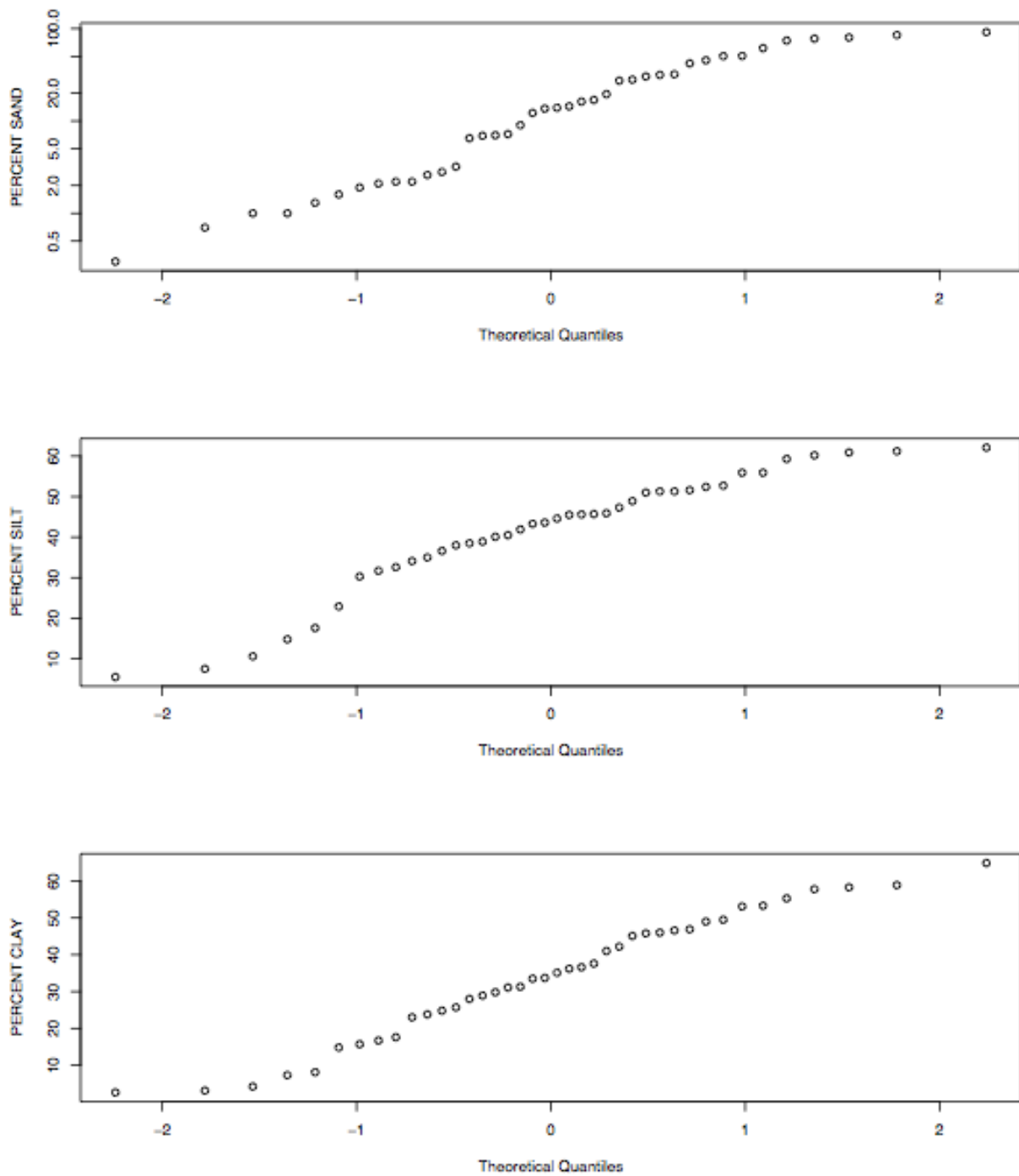


Figure 4. Cumulative frequency distributions (by quantiles of standard deviation or standard normals about the median) for sand, silt, and clay. Note that only the Percent-Sand ordinate is log scale and implies the sand distribution is log-normal while silt and clay distributions are normal (gaussian).

TABLE 1. Sand and Peat Bed Extent Based on Core Logs and Sand Content of Core Sub-Samples

	Lower Walnut Creek Reach			
	All	Lower	Middle	Upper
Percent Sand Beds	8.3	6.7	8.1	21.3
Percent Peat Beds	10.5	7.1	29.1	3.6
Other	81.2	86.2	62.8	75.1
Total Core Length, ft	179.4	131.6	31	16.9
Number of Sub-Samples	40	21	10	9
Percent w/ > 50% Sand	20	14.3	20	33.3
Mean Sand in Samples	24.3	16.7	28.7	37.3
Median Sand Sampled	13.8	7	16.6	32

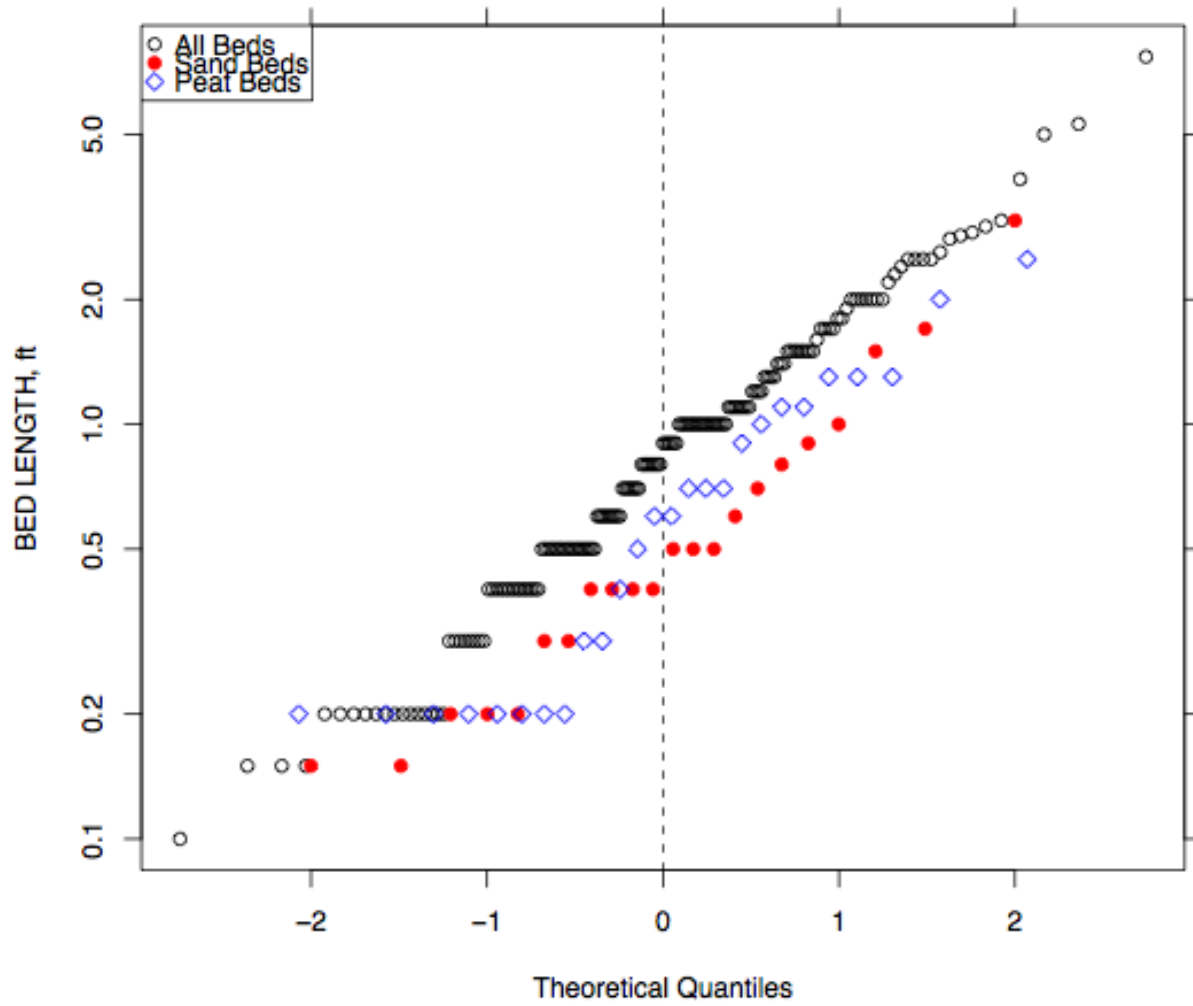


Figure 5. Distribution of all, sand, and peat bed lengths in sediment cores.

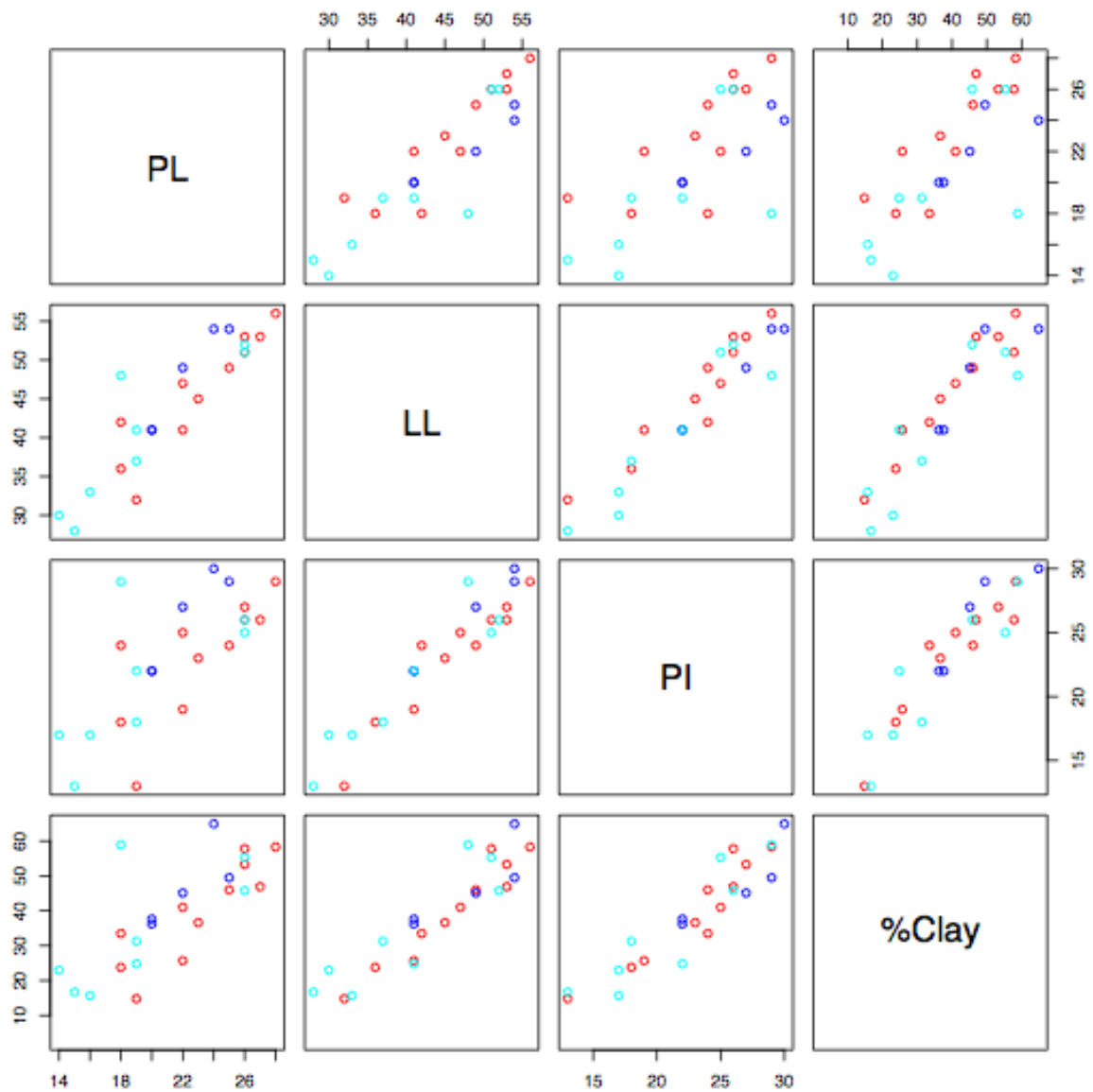


Figure 6. Scatter plots of Atterberg liquid limit (LL), plastic limit (PL) and plasticity index (PI, LL - PL) parameters, and clay fraction. Color coding is by sub-reach as described in Figure 1.

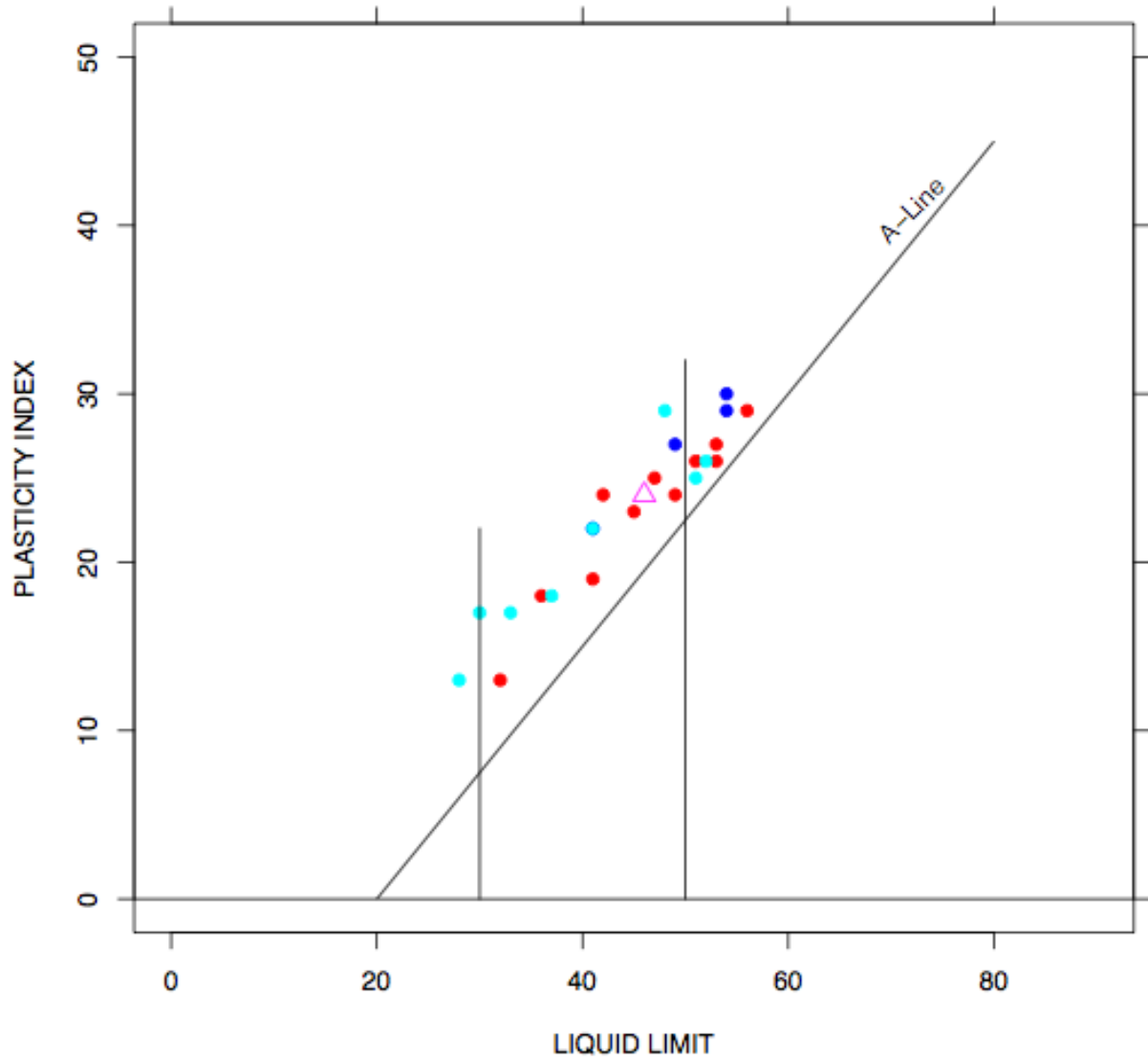


Figure 7. Plasticity graph of Atterberg data (dots) and dataset median values (maroon diamond) in relation with Casagrande's A-line indicating high resistance to erosion. Color coding of dots is by channel sub-reach as described in Figure 1.

TABLE 2. Summary of Measured and Derived Sediment Parameters				
Parameter	Mean	Median	16th Percentile	84th Percentile
<i>C_w</i> , %	57.4	56	49	69
<i>O_f</i> , %	2.9	3	2.3	3.6
PI, %	23	24	17.7	27.6
PL, %	21.6	22	18	26
LL, %	44.3	46	35	53
<i>TDS</i> , g/l	12.1	12	9.9	14.8
Clay, %	34.1	34.4	15.9	52.2
Silt, %	41.3	44.1	30.6	55.1
Sand, %	24.4	13.8	1.9	50.5
Gravel, %	0.25	0	0	0
Median D, μm	15.9	10.8	4.6	76.5
Mean D, μm	11.7	7.7	3.1	50.6
Sorting, μm	0.141	0.14	0.09	0.185
Skewness	-0.233	-0.23	-0.013	-0.362
<i>BWD</i> , kg/cu m	1556.6	1517.6	1426.6	1729.3
<i>C_s</i> , kg/cu m	910.1	849.9	699.1	1194.3
Moisture <i>w</i> , %	79.2	78.6	44.9	104.1

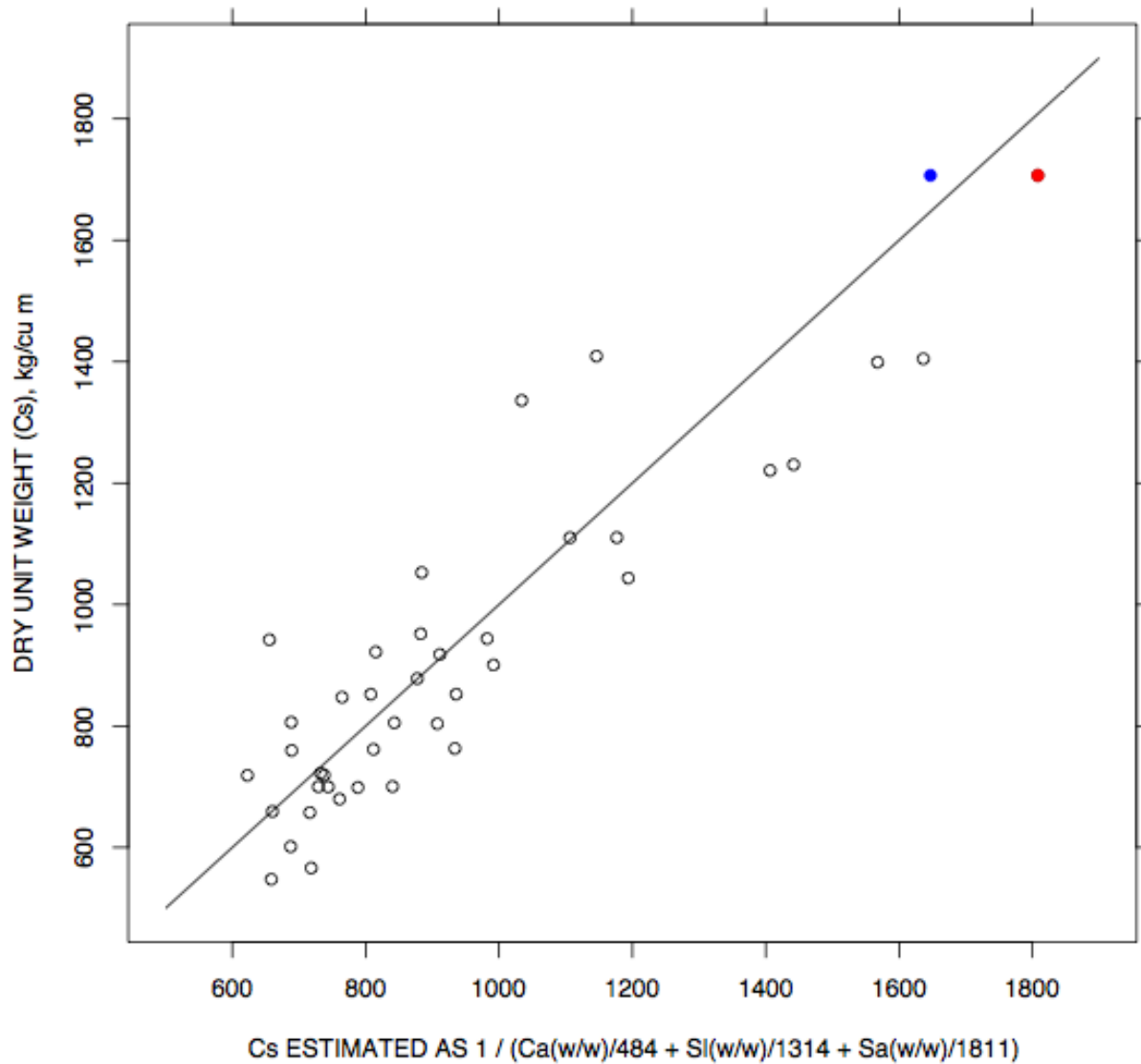


Figure 8. Unit dry weight measurements and estimates from clay Ca, silt Sl, and sand Sa grain mixes. Note that the red point in top right corner was computed from raw sand content while the blue point is the same sample computed by adding the gravel content (about 10 percent) to the sand.

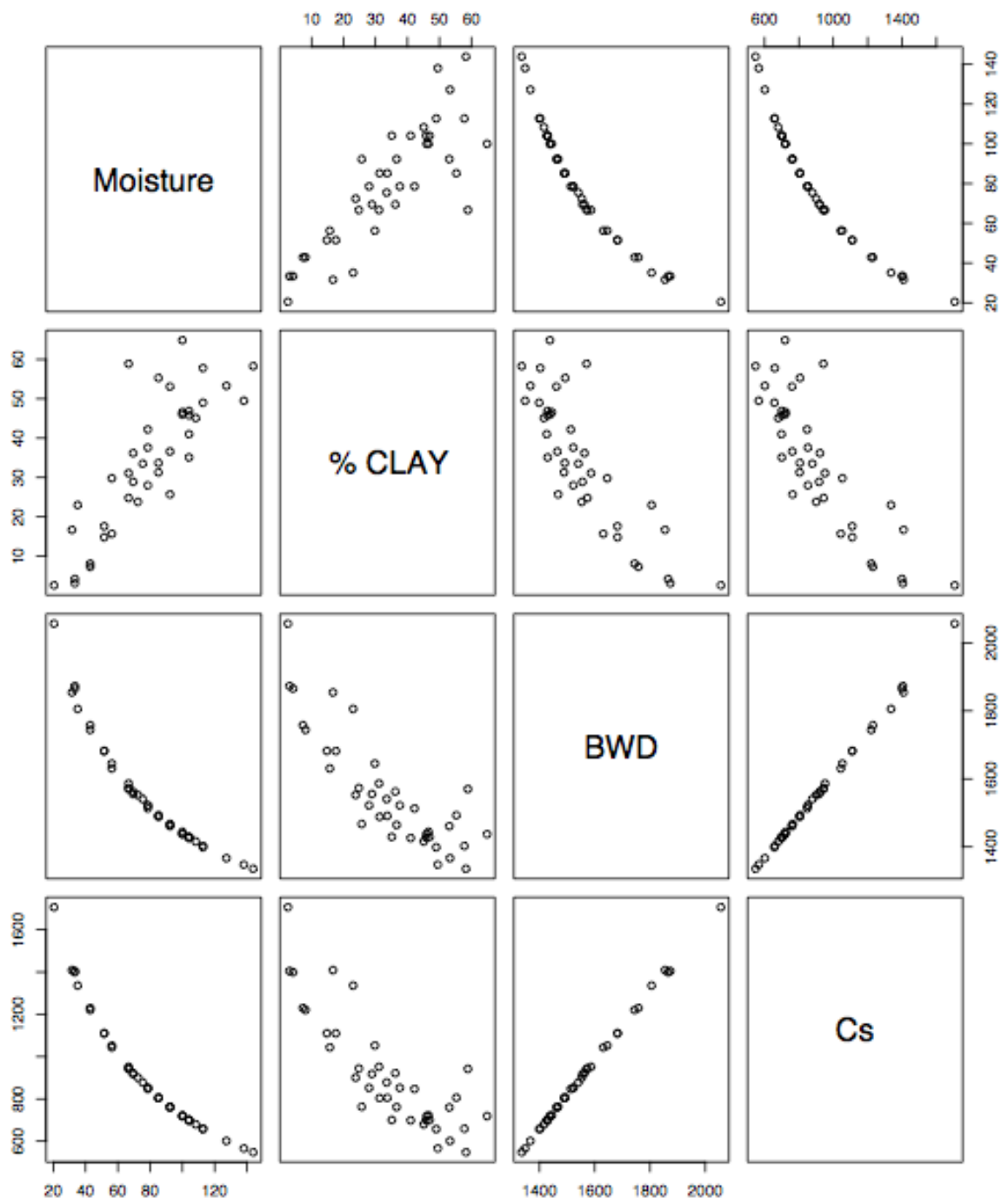


Figure 9. Scatter plots of concentration parameters and clay fraction.

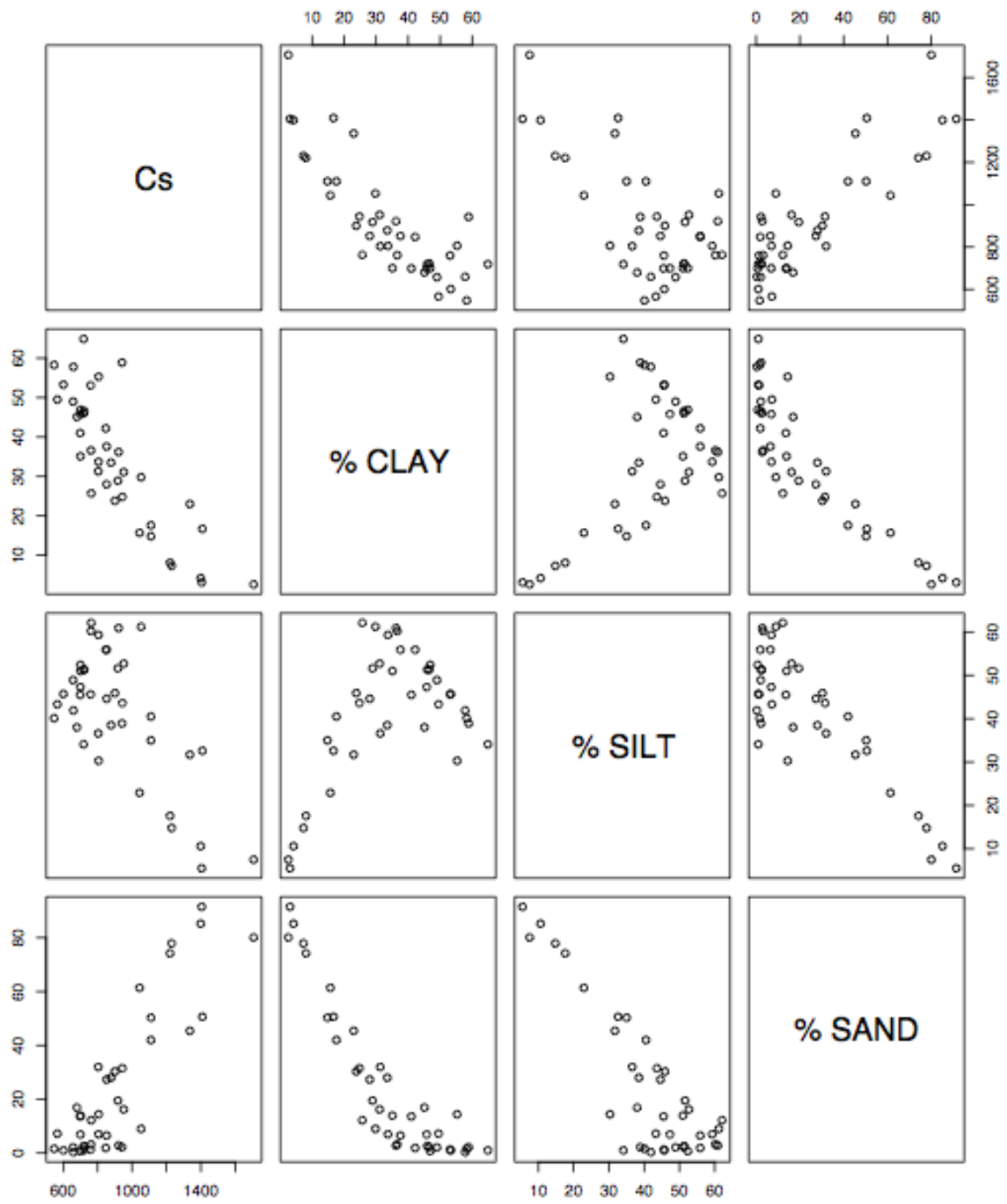


Figure 10. Scatter plots of clay, silt, and sand percentages and unit dry weight (solids content, kg/cu m).

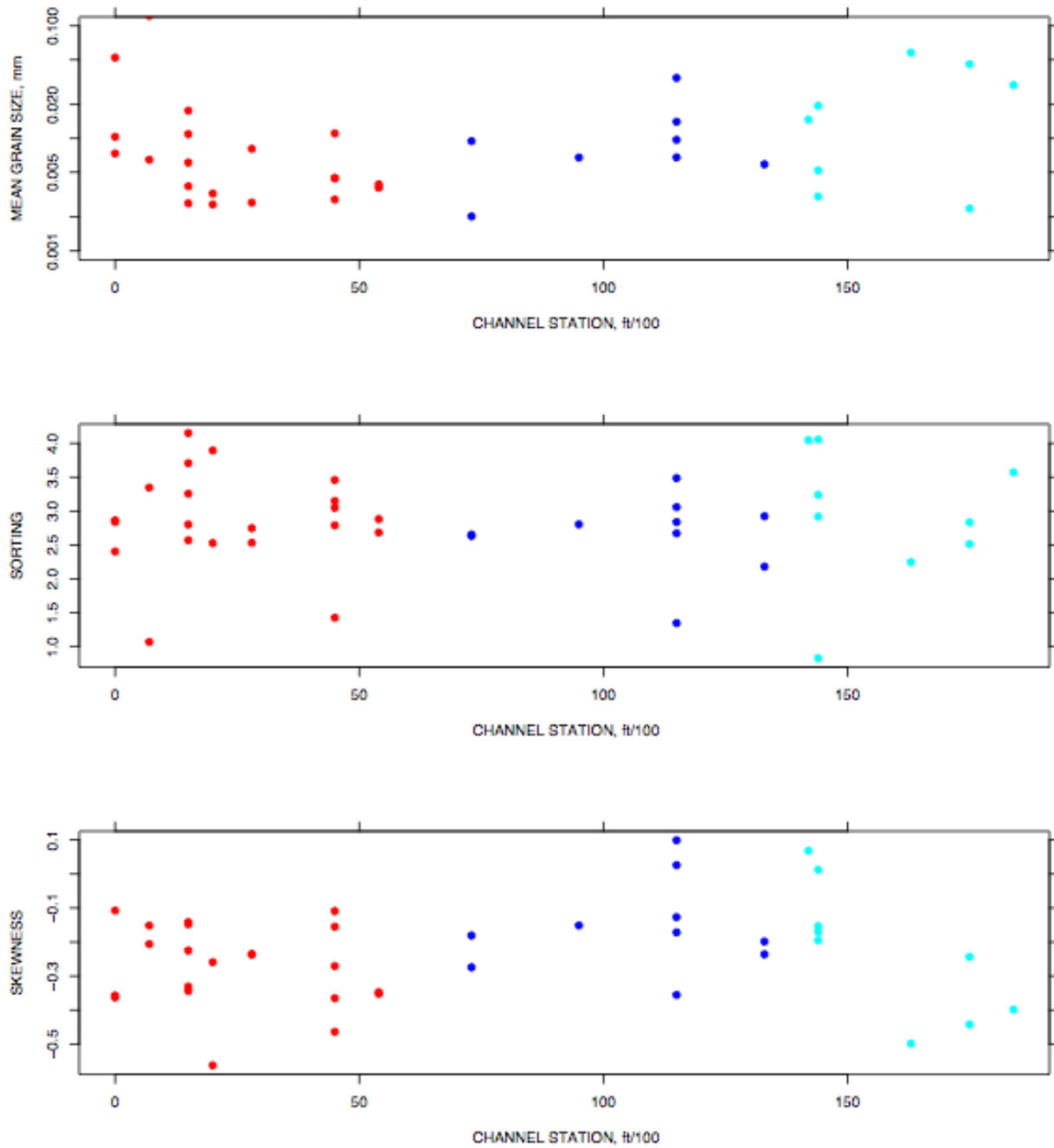


Figure 11. Grain size distribution statistics plotted by channel station. Color coding is as described for Figure 1.

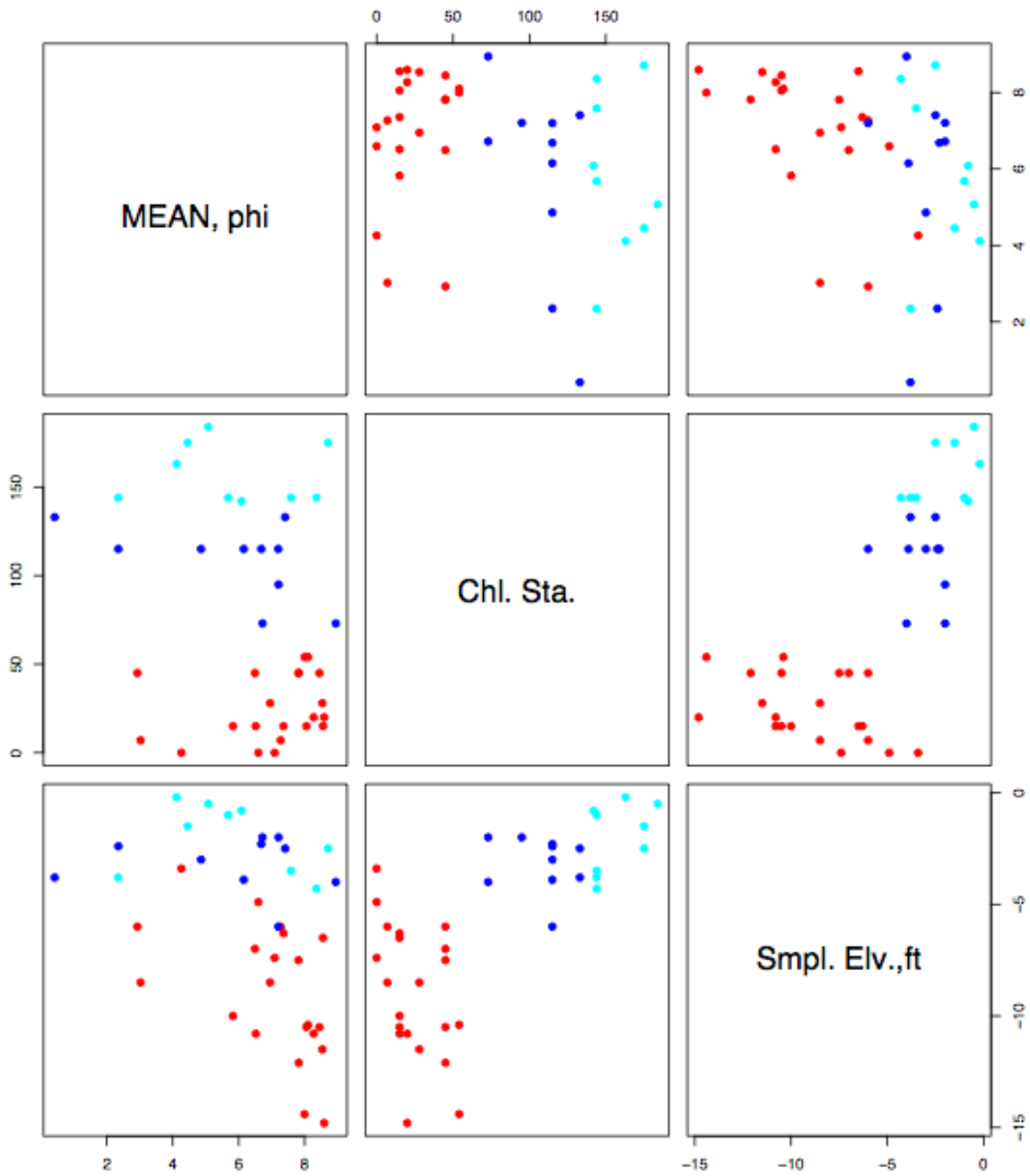


Figure 12. Scatter plots of mean grain size in phi-units (small values are larger sized), channel station (ft/100), and sample elevation (ft, mtl). Color coding is as for Figure 1 and 11.

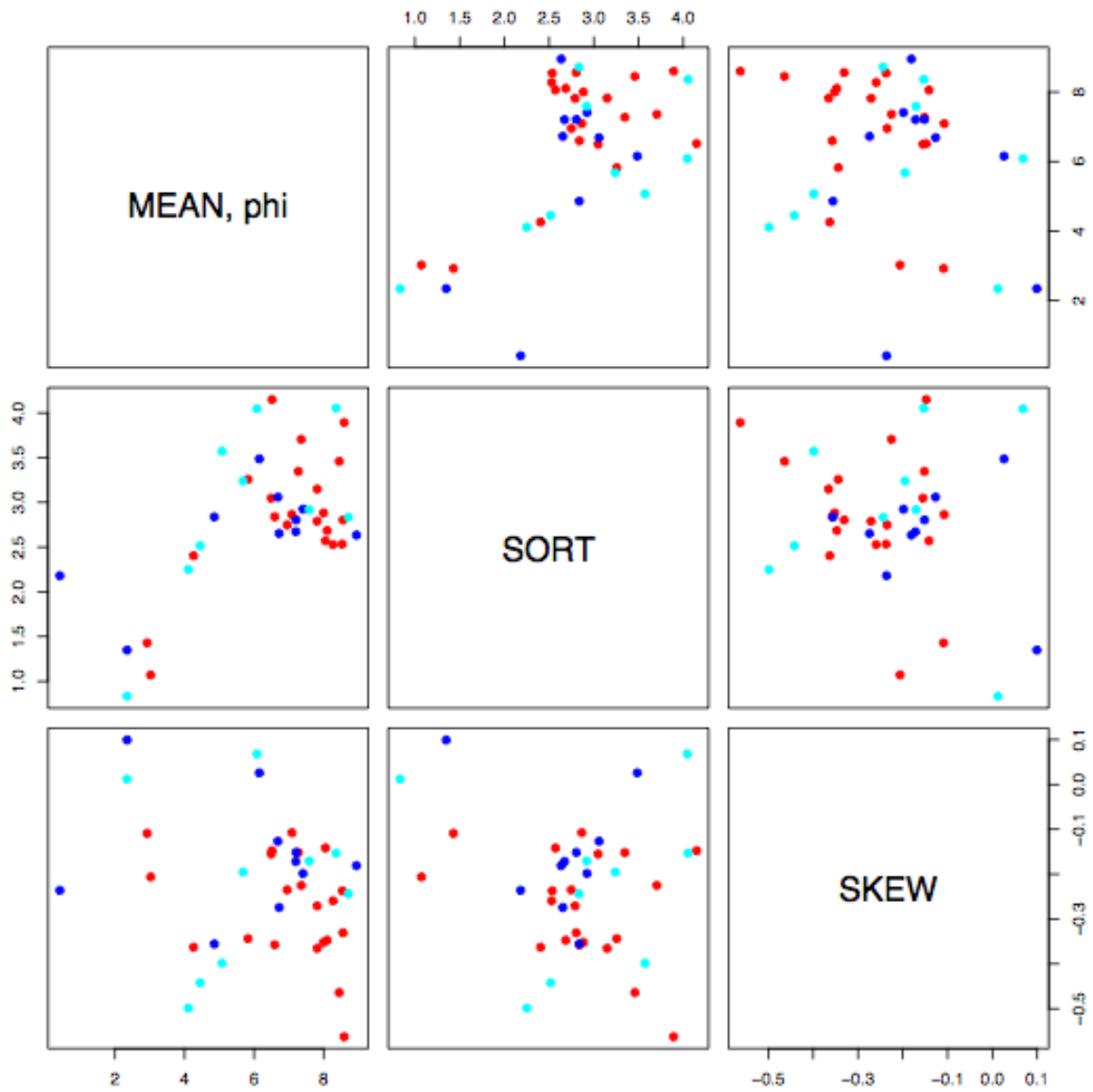


Figure 13. Scatter plots of mean grain size in phi-units (small values are larger sized), sorting, and skewness color coded by channel reach as described in Figure 1.

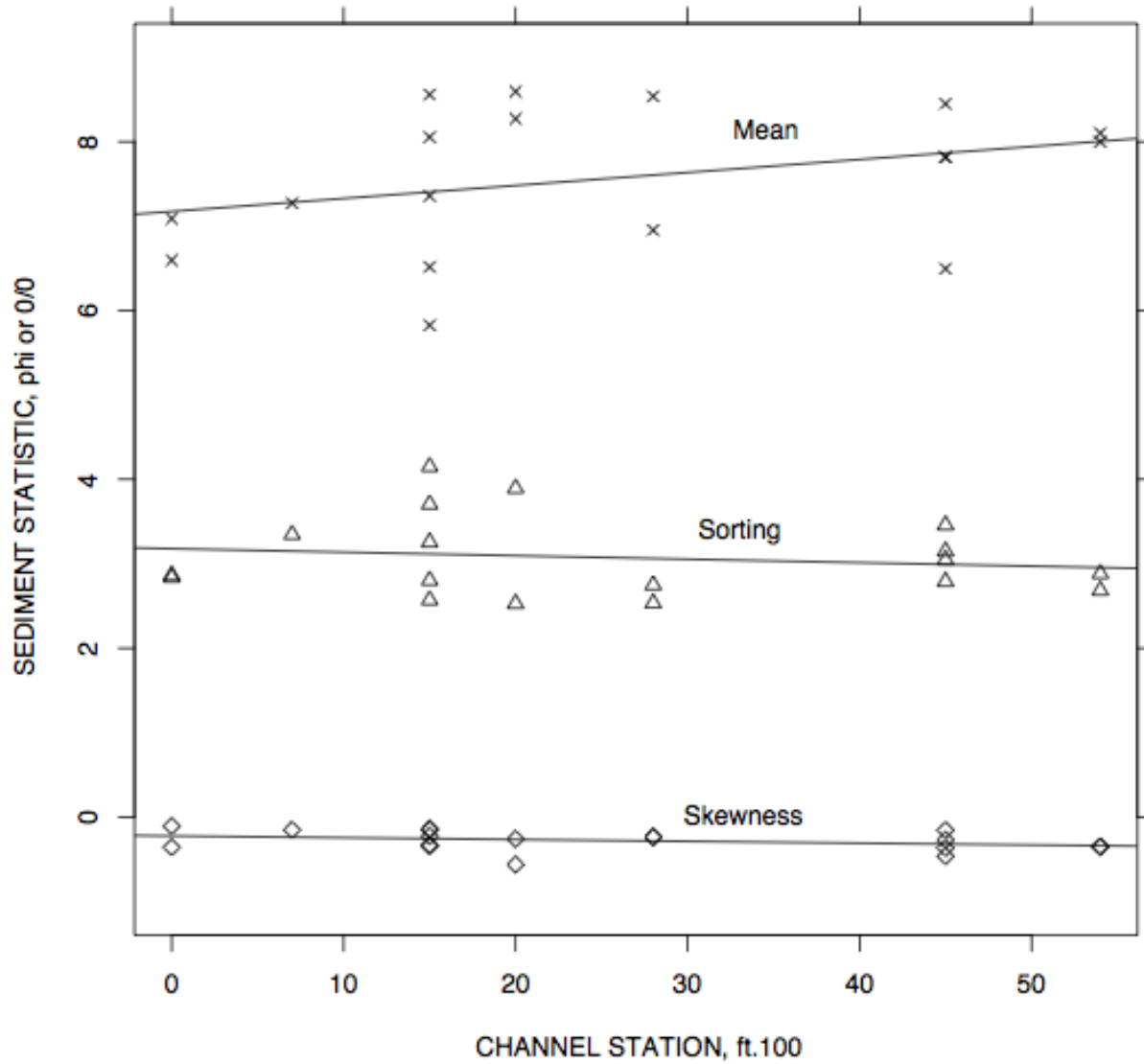


Figure 14. Lower project reach below Waterfront Road mean sediment phi size (x's where smaller numbers are larger sized), sorting (triangles), and skewness (diamonds) with least-squares trend lines.

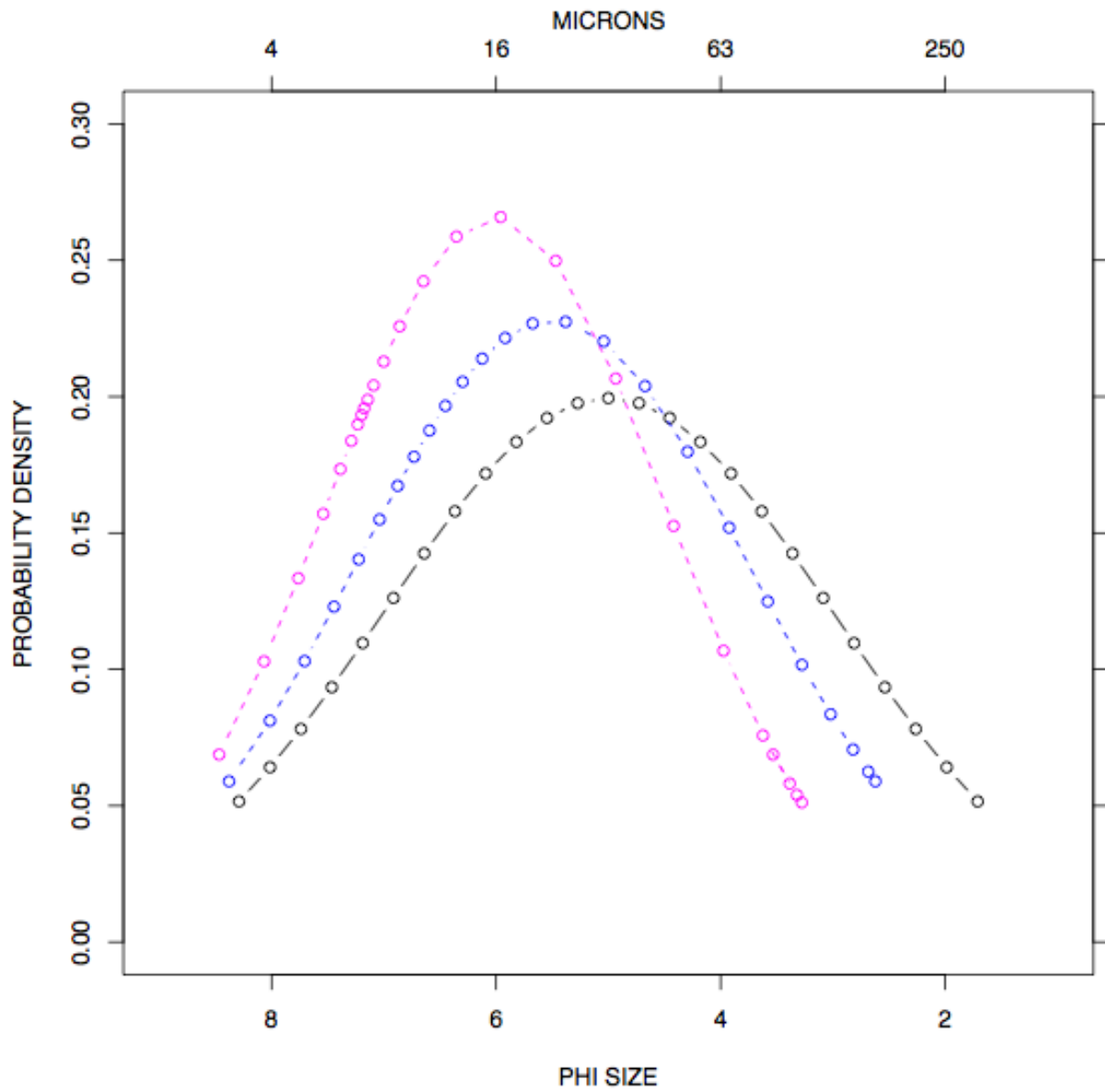


Figure 15. An example series of hypothetical differential grain-size distributions which become finer, more well sorted, and more skewed in the larger direction along a depositional path from black to blue to pink.

Sediment Transport Parameters

Sediment parameters were estimated based on previous laboratory studies of dredged material from the San Francisco Bay area⁷. Composites of maintenance dredged material from the bay area were tested by the WES Hydraulics Laboratory (POC Teeter) and by the University of Florida (POC Mehta). Those tests, taken together, indicated a two-phase particle erosion where erosion is first initiated at a low level of shear stress (Type I/II) and then increases more sharply at higher shear stress (Type II). These threshold stresses and erosion rate estimates were used to set active and inactive layers. Mass erosion occurs when the sediment matrix yields (the yield point) and increases sharply with clay solids content. A value was selected here (10 Pa) that is probably on the low side for this sediment column type and density. However, the mass erosion threshold for freshly deposited clay material would be expected to be about 6 Pa. Threshold shear stresses for deposition are from Krone's tests on bay sediments.

HEC-6 card fields are presented in the two tables that follow first in SI and metric units and then in HEC-6 units. The special I2 cards will have to be repeated after the I3 card. Thus, silt and clay will be transported together.

TABLE 3. HEC-6 Card Fields in SI Units				
Field	Card I2	Card I2 Spec. Active layer	Card I2 Spec. Inactive layer	CARD I3 Silt
2	MTCL =2	1	2	MTCL=2
3	ICS=1	DTCL=0.06 Pa	DTCL=0.06 Pa	IASL=1
4	LCS=1	STCD=1.0 Pa	STCD=1.0 Pa	LASL=4
5	SPGC=2.53	STME=10 Pa	STME=10 Pa	SPGC=2.53
6	DTCL=0.06 Pa	ERME=0.144 g/cm ² /min	ERME=0.144 g/cm ² /min	DTSL=0.08 Pa
7	-	ER2=60	ER2=60	-
8	PUCD=484 kg/m ³			PUSD=1314 kg/m ³
9	UWCL=484 kg/m ³			UWSL=1314 kg/m ³
10	CCCD=0			CCSD=0

⁷ Teeter, A.M. (1987.) "Alcatraz disposal site investigation; Report 3; San Francisco Bat-Alcatraz disposal site erodibility," Misc. Paper HL-86-1, USACE, Waterways Exp. Station, Vicksburg, MS.

Conversions: $1 \text{ kg/m}^3 = 0.06243 \text{ lbs/ft}^3$
 $1 \text{ Pa} = 1 \text{ N/m}^2 = 0.02089 \text{ lbs/ft}^2$
 $1 \text{ g/cm}^2/\text{min} = 122.918 \text{ lbs/ft}^2/\text{hr}$

TABLE 4. HEC-6 Card Fields in Required English Units				
Field	Card I2	Card I2 Spec. Active layer	Card I2 Spec. Inactive layer	CARD I3 Silt
2	MTCL =2	1	2	MTCL=2
3	ICS=1	DTCL=0.00125 lbs/ft ²	DTCL=0.00125 lbs/ft ²	IASL=1
4	LCS=1	STCD=0.0209 lbs/ft ²	STCD=0.0209 lbs/ft ²	LASL=4
5	SPGC=2.53	STME=0.2089 lbs/ft ²	STME=0.2089 lbs/ft ²	SPGC=2.53
6	DTCL=0.00125 lbs/ft ²	ERME=17.70 lbs/ft ² /hr	ERME=17.70 lbs/ft ² /hr	DTSL=0.00167 lbs/ft ²
7	-	ER2=60	ER2=60	-
8	PUCD=30.2 lbs/ft ³			PUSD=82.0 lbs/ft ³
9	UWCL =30.2 lbs/ft ³			UWSL=82.0 lbs/ft ³
10	CCCD=0			CCSD=0

The HEC-6 standard particle fall velocity for a clay particle 2 to 4 μm (geometric mean = 2.8 μm) is estimated to be 0.00762 mm/sec (2.5e-5 fps) using the FISC method (report 12, 1957). The grain size determinations and solids content included material as small as 0.5 μm or less. The geometric mean of the clay material determinations is therefore about 1.6 μm since the upper cutoff for clay was 5 μm .

Specifying a fall velocity for clay particles is made difficult by the fact that even in fresh water they exist in floccules of many particles⁸ - though not as large and dense as in seawater. The clay minerals in the Sacramento - San Joaquin river system and Suisun Bay are a mix of illite and montmorillonite⁹ which have a very high surface-area to volume ratio due to their platy-, sheet-like particle configuration. Such flocs are fragile and difficult to study because their size

⁸ Chase, R.R.P. (1979,) "Settling behavior of natural aquatic particles," *Limnol. Oceanogr.*, 24:3, pp. 417-426.

⁹ Knebel, H.J., Conomos, T.J., and Commeau, J.A. (1977.) "Clay-mineral variability in the suspended sediments of the San Francisco Bay system, California," *J. Sedim. Petrology*, 47:1, pp. 229-236.

and density depend on concentration, fluid shear rate in the water column, the presence of organic material, salinity, etc.

Previous laboratory tests on Detroit River sediment material 90 percent less than 10 μm in freshwater (with varied concentration and fluid shear rate) indicated an overall median floc fall speed of about 0.07 mm/sec at 20° C¹⁰. Laboratory tests of resuspended Atchafalaya Bay channel deposits with a median diameter of about 2 μm indicated a median fall speed of 0.020 to 0.016 mm/sec in river water.¹¹ The same study performed 30 field settling tests on bay water suspensions at low-current sites and found that sediment settling speed decreased away from the river mouth. The median setting speed was 0.04 mm/sec (25 and 75 percentile values were 0.009 and 0.07 mm/sec, respectively).

Based on representative observed clay fall speeds, a flocculation factor of 3-6 is recommended to be applied to the HEC-6 clay fraction fall speed. Some model sensitivity tests with factors in this range might be appropriate.

¹⁰ Burban, P.-Y., Xu, Y.-O., McNeil, J., and Lick, W. (1990.) "Settling speed of flocs in freshwater and seawater," J. of Geophys. Res., 95:C10, pp. 18,213-18,220.

¹¹ Teeter, A.M., and Pankow, W. (1989.) "The Atchafalaya River Delta; Report 2 Field data; Section 2: Settling characteristics of bay sediments," Techn. Rpt. HL-82-15, USACE, WES, Vicksburg, MS.